Pore-scale Simulation of Coupled Two-phase Flow and Heat Transfer through Dual-Permeability Porous Medium

H.A. Akhlaghi Amiri[1], A.A. Hamouda[*1]
[1]University of Stavanger (UiS), Department of Petroleum Engineering, 4036 Stavanger, Norway
*Corresponding author: aly.hamouda@uis.no

Abstract: This paper addresses one of the major challenges in water-flooded oil reservoirs, which is early water breakthrough due to the presence of high permeable layers in the media. COMSOL Multiphysics™ is used to model two phase (water and oil) flow in dual-permeability porous medium at micro-scales. The heat transfer module is coupled with the laminar two-phase flow interface, because temperature affects the flow patterns in the reservoir by modification of physical parameters. The specific heat and thermal conductivity are defined as functions of the order parameter, to take constant values in bulk phases and vary smoothly through the interface. Polymer injection, a remedy for the low sweep efficiency is simulated here by defining a variable viscosity for the aqueous phase that varies as a function of time and temperature. The simulation results confirm the efficiency of the polymer injection in enhancing oil recovery in dual-permeability porous medium.

Keywords: phase field method, heat transfer, dual-permeability, viscosity, temperature.

1. Introduction

One of the major challenges in the field of petroleum reservoir engineering is water conformance control in water-flooded reservoirs. Heterogeneities such as high permeable (thief) zones cause early water breakthrough, hence reservoir low sweep efficiency. A remedy for this problem is addition of polymers to the injected water. Polymer solution before activation flows with water through high permeability layers. Upon activation, the polymer network is formed causing the viscosity to increase. The high viscosity fluid preferentially flows through high permeable zone, hence increase the resistivity, allowing the flooding water to flow through low permeability zone and increase the sweep efficiency. Simulation of such a problem at pore-scale is the main objective of this paper.

It is useful to model flow problems at pore-scales to better comprehend transport phenomena in porous media. Pore-scale models can be used to derive macro-scale constitutive relations (e.g. capillary pressure and relative permeabilities) and to provide flow properties for simulation in larger scales [1]. Pore-scale simulation of fluid flow through porous media demands a method that can handle complex pore geometries and topological changes. Among other methods, phase field method (PFM), which is categorized as interface capturing approach, is becoming increasingly popular because of its ability to accurately model flow problems involving sophisticated moving interfaces and complex topologies [2].

The first idea of PFM (also known as diffuse-interface method) goes back to a century ago when van der Waals modeled a liquid-gas system using a density function that varies continuously at the interface. Convective Cahn-Hilliard equation [3] is the best known example of PFM that can conserve the volume and is relatively easy to implement in two and three dimensions [4]. During the last decade, different applications of Cahn-Hilliard PFM in simulation of two-phase Navier-Stokes flows have been suggested [5-7].

Temperature is an important parameter that plays a key role in the reservoir. It affects the flow patterns through modifications of physical parameters. So in order to include the effect of temperature, it is necessary to couple heat transfer model with two-phase flow (phase field) model. To accurately implement this coupling, COMSOL Multiphysics™ is used in this work. It is an interactive environment capable of coupling between different scientific and engineering problems. It uses finite element method (FEM) to solve the equations. The software runs finite element analysis together with error control using a variety of numerical solvers. In present work, 2D flow problems are modeled using Cahn-Hilliard PFM coupled with heat transfer.

2. Governing Equations

Cahn-Hilliard convection equation is a time dependent form of the energy minimization concept. It is obtained by approximating interfacial diffusion fluxes as being proportional to chemical potential gradients, enforcing conservation of the field [8]. This equation models creation, evolution and dissolution of the interface:

$$\frac{\partial \phi}{\partial t} + u.\nabla \phi = \nabla .(M \nabla G) \quad (1)$$

where ϕ is a representative of the concentration fraction of the two components and is called order parameter. It takes distinct constant values in the bulk phases (e.g., -1 and 1) and varies rapidly between the constant values across the interface. M is the diffusion coefficient called mobility that governs the diffusion-related time scale of the interface and G is the chemical potential of the system. Mobility can be expressed as $M = M_c \varepsilon^2$, where M_c is the characteristic mobility that governs the temporal stability of diffusive transport and ε is a capillary width that scales with the interface thickness. The chemical potential is obtained from total energy equation as $G = \lambda \left[\phi \ (\phi^2 - 1) / \varepsilon^2 - \nabla^2 \phi \right]$, where λ is the mixing energy density. Equation (1) implies that the temporal evolution of ϕ depends on convective transport due to the divergence free velocity and diffusive transport due to gradients in the chemical potential [9].

To simulate immiscible two phase flow problems, equation (1) is coupled with the incompressible Navier-Stokes and continuity equations with surface tension and variable physical properties as follow:

$$\rho \frac{\partial u}{\partial t} + \rho \, u.\nabla u = -\nabla p + \nabla .\left[\mu (\nabla u + \nabla u^T) \right] + F_{st} \quad (2)$$

$$\nabla .u = 0 \quad (3)$$

where p is pressure, ρ is density, μ is viscosity and F_{st} is the surface tension body force. The viscosity and density are defined as functions of order parameter, hence

$$\mu = (\mu_2 - \mu_1) \times (1 + \phi)/2 + \mu_1 \quad (4)$$

$$\rho = (\rho_2 - \rho_1) \times (1 + \phi)/2 + \rho_1 \quad (5)$$

where subscript 1 and 2 denote different phases. Surface body force is calculated by derivation of the total free energy due to the spatial coordinate which is obtained as follows [10]:

$$F_{st} = G \nabla \phi \quad (6)$$

PFM considers surface tension as an intrinsic property corresponding to the excess free energy density of the interfacial region [11]. Surface tension coefficient for PFM is equal to the integral of the free energy density across the interface, which is $\sigma = 2\sqrt{2}\lambda / (3\varepsilon)$ in the case of a planar interface.

To include the effect of temperature in the model, heat equation must be also coupled with the interface equation (1) and momentum and continuity equations (2) and (3). Heat equation for fluids, which includes convective and conductive heat transfers, is obtained as follows:

$$\rho C_p \frac{\partial T}{\partial t} + \rho C_p u.\nabla T = \nabla .(k \nabla T) \quad (7)$$

where T is the absolute temperature, C_p is the specific heat capacity and k is the thermal conductivity. C_p and k are defined as functions of order parameter to get constant values in the bulk phases and smoothly vary through the interface (see Table 1).

The built-in laminar two phase flow and heat transfer modules of COMSOL Multiphysics are used to carry out the numerical simulations. The two interfaces are coupled by COMSOL using the coupling parameters of the velocity field (u), pressure (p) and temperature (T).

2. Geometries and Numerical Schemes

The 2D porous media are computed by subtracting the circular grains from the rectangular domains. The circular grains are represented by an equilateral triangular array. The area of the domain is 15×4.6 mm^2. The grain radius and throat width determines the porosity and hence the permeability of a medium. In the homogenous porous medium (Figure 1a), all the grains have the same radius of 0.5 *mm* and the

throat width is 0.15 *mm*. However, in the dual-permeability medium (Figure 1b), the grains have two different radiuses of 0.5 and 0.4 *mm*. The pore throat width is 0.15 and 0.35 *mm* in low and high permeability zones, respectively. With this geometry, the permeability contrast in this medium is approximately 10. No-slip boundary conditions are used for the grain walls. In other words, the fluid-grain contact angle is set to $\pi/2$ (i.e., neutral wettability). Symmetry boundary conditions are imposed on all the lateral sides, extending the geometry in the lateral directions. The model is initially saturated with phase 1 (oil) and phase 2 (water or polymer solution) is injected with constant low velocity from the inlets on the left hand side of the model. The two phases can flow out through the outlets, located on the right hand side of the media. The outlet is kept at zero pressure.

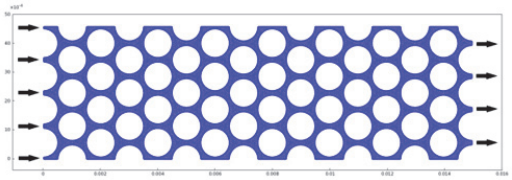

a

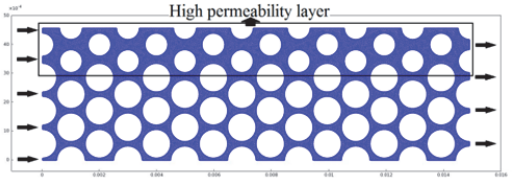

b

Figure 1. The geometries of a) homogenous and b) dual-permeability porous media for two-phase flow modeling.

In heat transfer simulation, to model the thermal effects of solid grains in the porous media, the circular grains are added to the dual-permeability domain (Figure 2). The module of heat transfer in solids is applied to the grains. The physical properties of sandstone are used for the grains (see Table 1). The initial temperature of the medium and the oil is T_0=90 ^{o}C (363.15 K). Water is injected with the initial temperature of T_{in}=20 ^{o}C (293.15 K). To simulate the thermal infinity around the model, the outer surfaces of the grains on the boundary are kept at T_0. Symmetry boundary conditions are imposed on all the lateral sides, extending the heat transfer model in lateral directions.

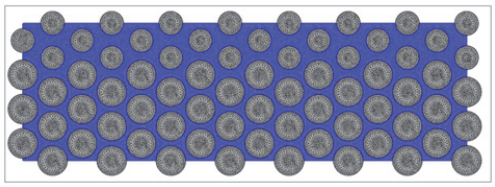

Figure 2. The geometry of the dual-permeability domain that contains both the porous medium and the grains for heat transfer modeling.

Uniform triangular mesh elements are applied in all the computations of the present work. To avoid unphysical distortions and to make sure about the accuracy of the results, the interface is made thin enough to approach sharp interface limit. On the other hand, the interface region is adequately resolved by fine meshes. These criterions are called model convergence and mesh convergence, respectively [12]. Mobility (M) is another important parameter that affects the accuracy of the phase field method [4]. Mobility has to be large enough to retain the constant interface thickness and small enough to keep the convective motion [10]. Several sensitivity studies were performed to obtain the optimum interface thickness, mesh sizes and mobility. The time steps sizes are controlled during the computations by numerical solver, in order to make the solution convergence easier. Particularly, the initial time step sizes are very small to avoid singularity. Standard boundary conditions are used in the simulations. Boundary conditions for different cases under consideration will be specified in due place during their specification.

3. Results and Discussion

3.1 Effects of Viscosity and Permeability Contrasts

In a displacement process through a porous medium, if the medium is homogenous and the viscosity of the displaced fluid (μ_1) is equal to or less than that of the injected fluid (μ_2), the displacement process is stable. Figure 3a illustrates the fluid distribution at a time during the displacement for a homogenous porous medium when $\beta = \mu_2/\mu_1 \geq 1$. This stable process is called piston-like displacement. The

velocity field (Figure 3b) is distributed homogenously in the medium, i.e., both fluids have equal maximum velocities in the pore throats and equal minimum velocities in vicinity of the grains inside the pores. Ideally, the piston-like displacement can fully recover the fluid inside the medium. However, if $\beta << 1$ or there is a high permeable zone in the porous medium, the sweep efficiency declines due to the early breakthrough of the displacing phase.

When the injected fluid (water) is less viscous compared to the displaced fluid (oil), it may show front instabilities, even in homogenous porous media. This is called fingering, a particular case of Rayleigh-Taylor instability well-known in fluid dynamics. It takes place when the displacing phase is more mobile (less viscous) than the displaced phase. Water fingers propagate through the media leaving clusters of the oil behind. Starting time, number and thickness of the fingers are related to the viscosity ratio as well as the injection rate. To be able to see this phenomenon in our small medium, the injection velocity is set to a very low value and the viscosity contrast is set to $\beta = 0.01$. Figure 4a shows the fingering phenomenon in the homogenous porous medium. The water flows just through the finger as is demonstrated in the velocity filed in Figure 4b.

On the other hand, when there is a high permeable layer in the medium, it is first swept by the injected fluid, as shown in Figure 5a. Because higher permeability zone possesses lower flow resistivity and the fluids have tendency to flow through lower resistive area. This layer creates a path toward the outlet, which results in an early breakthrough of the injected fluid. After breakthrough, all the injected fluids flow directly through this path (Figure 5b) and other parts of the medium remain unswept.

To increase the sweep efficiency, a first order solution is to add polymer to the injected water. Polymer solution has initial water viscosity and flows directly through the water paths. As it is activated by temperature, the viscosity of the polymer solution increases, causing high resistivity zone in front of the water which has been flooded after the polymer. Hence the water is diverted to the low permeability zone. This process is simulated for dual-permeability porous medium in the coming section.

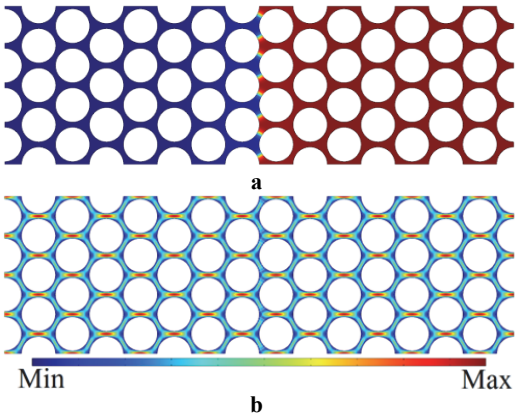

Figure 3. a) phase distribution and b) velocity field at a certain time during a piston-like displacement in the homogenous porous medium.

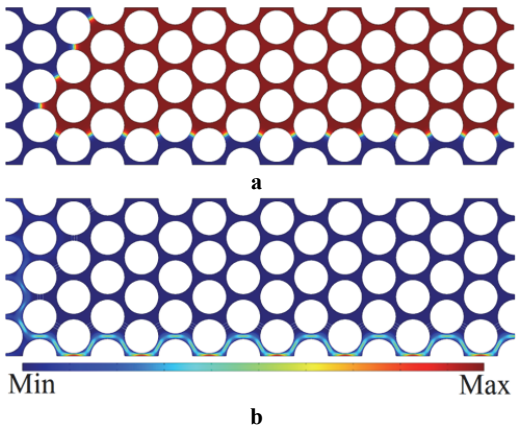

Figure 4. a) phase distribution and b) velocity field after stabilization in the homogenous porous medium when $\beta = 0.01$ (water fingering).

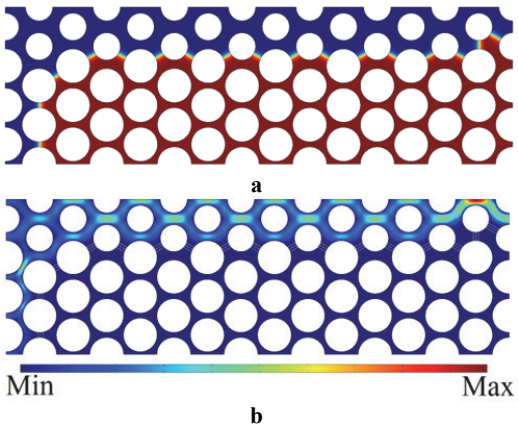

Figure 5. a) phase distribution and b) velocity field after stabilization in the dual-permeability porous medium when $\beta = 1$.

3.2 Simulation of Polymer Injection in Dual-Permeability Porous Medium

As discussed above for dual-permeability porous medium, after water breakthrough the flow pattern is stabilized and no more oil is produced (Figure 5). This is the time for polymer treatments. As polymers are strongly affected by the temperature, it is necessary to find the temperature gradient inside the medium before their application, especially when an in-depth activation is intended. To simulate the thermal interactions in our model, the heat transfer module is coupled with the two-phase flow interface with the boundary and initial conditions explained in section 2. The physical properties used in the heat transfer model are summarized in Table 1. Figure 6 illustrates the temperature profile corresponding to the flow pattern depicted in Figure 5. Figure 6 shows that after water breakthrough, there is a stabilized temperature gradient, mostly in the high permeable layer. It is deduced from the temperature profile that a polymer with the activation temperature of T_{act}=70 °C (343.15 K) can be activated approximately in the middle of the medium.

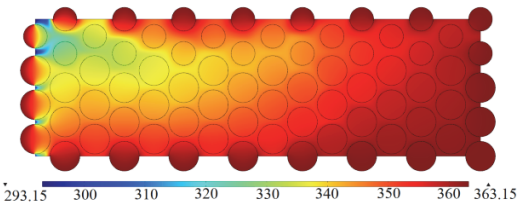

Figure 6. Temperature field after stabilization (4.5 *s*) in the dual-permeability porous medium ($\mu_2 = \mu_1 = 1\,cp$).

The polymer injection and activation are simulated by defining water viscosity that contains multiple step functions for time and temperature (see Table 1). The step location for time (polymer injection time) is at t=5 s, i.e., 1 *s* after breakthrough time (4 *s*), to let the fluid and temperature to be stabilized. The step location for temperature (activation temperature) is set to T_{act}. So the polymer is injected at *t*=5 *s* and is activated as it reaches $T_{act.}$ As a result of activation, the viscosity of water phase increases from 1 to 25 *cp*. The viscosity profile of water at *t*=5 *s* is demonstrated in Figure 7a. A high viscous bank is created in front of the high permeable layer, which increases the resistivity inside this region. The aqueous phase that is injected later will be diverted to the low permeable areas (Figure 7b). Figure 8 shows the fluid profiles at two moments after polymer injection. Water displaces the oil in the lower permeable zone toward the outlet.

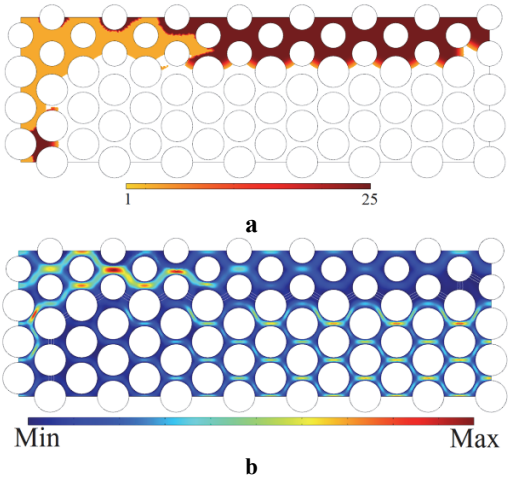

Figure 7. a) Viscosity of the aqueous phase and b) velocity filed after polymer activation in the dual-permeability porous medium.

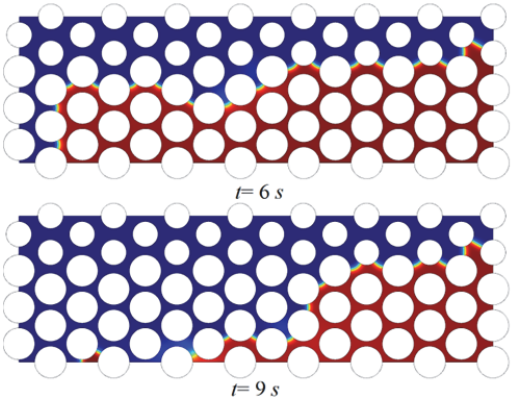

Figure 8. Fluid distributions in the dual-permeability porous medium at two moments after polymer activation.

The pressure profile inside the high permeable layer is studied at three different moments: before water breakthrough, after water breakthrough and after polymer injection (Figure 9). Before breakthrough time, there is a pressure jump between the two phases due to the surface tension. The pressure gradient inside each phase is very small. After breakthrough, water fills the high permeable layer and a linear pressure

gradient between the inlet and the outlet is created. When polymer is injected it is activated in the front half of the high permeable layer and the back half still remains low viscous. The front viscous bank has a higher pressure gradient due to its higher flow resistivity. Figure 10 shows that as a result of polymer injection, finally almost all the oil in the medium is recovered after 14 *s*. The recovery stops at less than 50% if the polymer treatment is not performed.

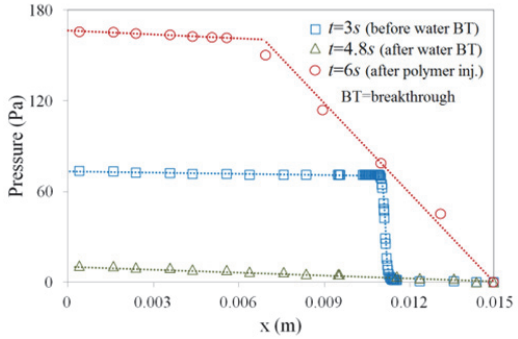

Figure 9. Pressure profile inside the high permeable zone versus distance from the inlet, at three different moments during the displacement process.

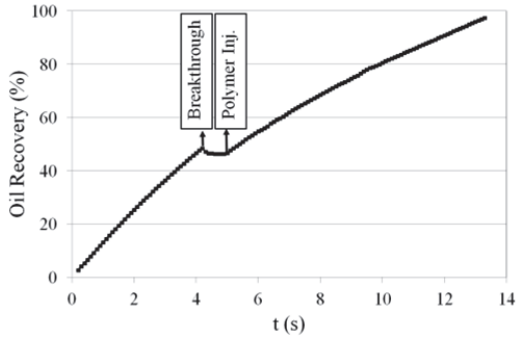

Figure 10. Oil recovery versus time for the dual-permeability porous medium.

4. Conclusions

In this work, COMSOL Multiphysics was used to solve the coupled two-phase flow and heat transfer at pore scale. The effect of permeability contrast in lowering the water sweep efficiency in the porous media was studied. The simulation of polymer injection in dual-permeability porous medium showed that proper polymer treatment enhances the oil recovery by creating high resistivity in the high permeable zone.

5. References

1. P.H. Valvatne, M.J. Blunt, Predictive pore-scale modeling of two-phase flow in mixed wet media, *Water Resources Research,* **40** (2004)
2. P. Yue, J.J. Feng, C. Liu, J. Shen, A diffuese interface method for simulating two-phase flows of complex fluids, *Journal of Fluid Mechanics*, **515**, 293-317 (2004)
3. J.W. Cahn, J.E. Hilliard, Free energy of a nonuniform system, *Journal chemical Physics*, **28 (2)**, 258-267 (1958)
4. D. Jacqmin, Calculation of two-phase Navier-Stokes flows using phase field modeling, *Journal of Computational Physics*, **155**, 96-127 (1999)
5. C. Liu, J. Shen, A phase field model for the mixture of two incompressible fluids and its approximation by a Fourier- spectral method, *Physics D*, **179**, 211-228 (2003)
6. P.H. Chiu, Y.T. Lin, A conservative phase field method for solving incompressible two phase flows, *Journal of Computational Physics*, **230**, 185-204 (2011)
7. I. Bogdanov, S. Jardel, A. Turki, A. Kamp, Pore scale phase field model of two phase flow in porous medium, Annual COMSOL Conference, Paris, France (2010)
8. V.E. Badalassi, H.D. Cenicerob, S. Banerjee, Computation of multiphase systems with phase field models, *Journal of Computational Physics*, **190**, 371-397 (2003)
9. A.A. Donaldson, D.M. Kirpalani, A. Macchi, Diffuse interface tracking of immiscible fluids: improving phase continuity through free energy density selection, *International Journal of Multiphase Flow*. **37**, 777-787 (2011)
10. P. Yue, C. Zhou, J.J. Feng, C.F. Ollivier-Gooch, H.H. Hu, Phase-field simulations of interfacial dynamics in viscoelastic fluids using finite elements with adaptive meshing, *Journal of Computational Physics*, **219**, 47–67 (2006)
11. R.S. Qin, H.K. Bhadeshia, Phase field method, *Material Science and Technology*, **26**, 803-811 (2010)
12. C. Zhou, P. Yue, J.J. Feng, C.F. Ollivier-Gooch, H.H. Hu, 3D phase-field simulations of interfacial dynamics in newtonian and viscoelastic fluids, *Journal of Computational Physics*, **229**, 498–511 (2010)

6. Acknowledgements

Authors acknowledge Dong Energy Company, Norway for the financial support and COMSOL support center for their technical guidance in the simulations.

Table 1: Physical properties of water, oil and grain (sandstone) used in the heat transfer simulation

Prop.	Value	Unit
C_p	$C_p = (C_{p-water} - C_{p-oil}) \times (1+\phi)/2 + C_{p-oil}$	J/kg.K
$C_{p\text{-}water}$	4200	J/kg.K
$C_{p\text{-}oil}$	2000	J/kg.K
$C_{p\text{-}grain}$	800	J/kg.K
k	$k = (k_{water} - k_{oil}) \times (1+\phi)/2 + k_{oil}$	W/m.K
k_{water}	0.6	W/m.K
k_{oil}	0.2	W/m.K
K_{grain}	2	W/m.K
ρ	$\rho = (\rho_{water} - \rho_{oil}) \times (1+\phi)/2 + \rho_{oil}$	Kg/m^3
ρ_{water}	1000	Kg/m^3
ρ_{oil}	1000	Kg/m^3
ρ_{grain}	2000	Kg/m^3
μ	$\mu = (\mu_{water} - \mu_{oil}) \times (1+\phi)/2 + \mu_{oil}$	Pa.s
μ_{water}	$0.001 + 0.024 \times U(t-5) \times U(T-343.15)$ U: Unit step function	Pa.s
μ_{oil}	0.001	Pa.s
σ	0.04	N/m